International Journal of Mechanical, Industrial and Aerospace Sciences
ISSN: 2517-9950
Vol:9, No:7, 2015

Design and Fabrication of an Array Microejector Driven by a Shear-Mode Piezoelectric Actuator

Chiang-Ho Cheng, Hong-Yih Cheng, An-Shik Yang, Tung-Hsun Hsu

***Abstract*—**This paper reports a novel actuating design that uses the shear deformation of a piezoelectric actuator to deflect a bulge-diaphragm for driving an array microdroplet ejector. In essence, we employed a circular-shaped actuator poled radial direction with remnant polarization normal to the actuating electric field for inducing the piezoelectric shear effect. The array microdroplet ejector consists of a shear type piezoelectric actuator, a vibration plate, two chamber plates, two channel plates and a nozzle plate. The vibration, chamber and nozzle plate components are fabricated using nickel electroforming technology, whereas the channel plate is fabricated by etching of stainless steel. The diaphragm displacement was measured by the laser two-dimensional scanning vibrometer. The ejected droplets of the microejector were also observed via an optic visualization system.

***Keywords*—**Actuator, nozzle, microejector, piezoelectric.

I. Introduction

THE piezoelectric ceramic is extensively adopted used in the solid-state actuator, which is designed for numerous applications, such as micropositioning mechanism [1], [2] and microdroplet-ejecting technology [3]–[9]. Ink jet printing is the most valuable application of microdroplet-ejecting technology. The commercial piezoelectric ink jet printing technologies are divided into four actuating modes according to the deformation of piezoelectric actuators. These modes, called bend [3], push [4], squeeze [5] and shear [6]–[9], are all designed to change the volume in the pressure chamber or flow channel and eject droplets from the orifice. For the bend mode illustrated in Fig. 1 (a), the diaphragm with the attached piezoelectric actuator is deflected inwardly into the pressure chamber due to the extension difference between the two layers. In the push mode illustrated in Fig. 1 (b), the piezoelectric rod pushes the diaphragm by its extension effect. In the squeeze mode illustrated in Fig. 1 (c), the radially polarized piezoelectric tube provided with the actuating electrodes on its inner and outer surface is considered as the pressure chamber, and its squeeze effect enables droplet ejection. The Xaar-type and Spectra-type inkjet heads designed, respectively, by the Xaar and Spectra companies, as shown in Figs. 1 (d1) and (d2), are well-known examples of shear-deformation piezoelectric actuators. In the Xaar-type design, the poled piezoelectric plate is micromachined to form a flow channel with the channel walls polarized along the wall-standing direction. An external electrical field applied along the wall-thickness direction is perpendicular to the polarization direction, causing shear deformation of the channel wall, resulting in a change of volume. In the Spectra design, a piezoelectric plate is poled along the thickness direction, and the actuating electrode pairs on the top surface impose an electric field orthogonal to the direction of polarization. The resulting shear deformation of the actuator reduces the volume of the pressure chamber and thus ejects a liquid drop from the orifice.

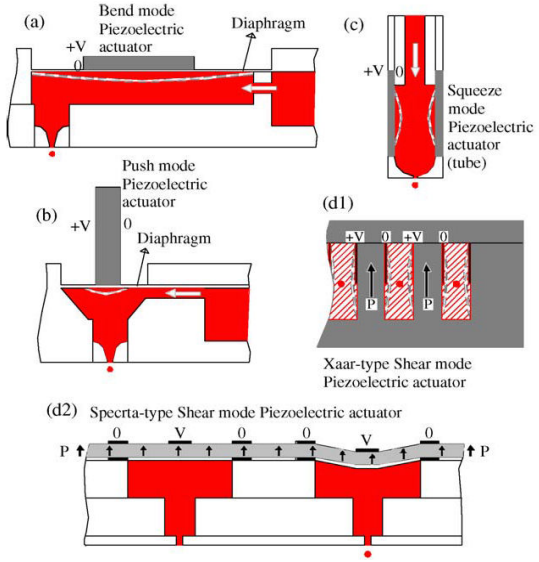

Fig. 1 Various deformation modes of piezoelectric actuators for inkjet printing technology

In this study, the novel actuating module consists of the shear mode piezoelectric actuator and the vibration plate with the feature of bulge diaphragm shown in Fig. 2. The bulge diaphragm is shaped with a piled-up bulge on the diaphragm. The shear mode piezoelectric actuator is glued onto the vibration plate, and its center area is placed on the bulge. The active region of the actuator is simply suspended, and the diaphragm can be deflected through the bulges, resulting in a sudden decrease in the chamber volume and causing droplets to be expelled from the orifice. Comparing to the above-mentioned actuators, this actuating design is advantaged

Chiang-Ho Cheng and Tung-Hsun Hsu are with the Department of Mechanical and Automation Engineering, Da-Yeh University, Changhua, 515, Taiwan (phone: (886)4-8511888 ext. 2119; e-mail: chcheng@mail.dyu.edu.tw).

Hong-Yih Cheng is with the Department of Mechanical and Automation Engineering, Da-Yeh University, Changhua, 515, Taiwan (e-mail: honyi@mail.dyu.edu.tw).

An-Shik Yang is with the Department of Energy and Refrigerating Air-Conditioning Engineering, National Taipei University of Technology, Taipei, 106, Taiwan (e-mail: asyang@ntut.edu.tw).

by the displacement enhancement and the uniformity at central region. The shear displacement is directly proportional to the polarization length. Hence, if a long-distance poled beam actuator is suspended on the larger range between the bulge and the outer area, then the displacement of the diaphragm is more enhanced and uniform. Consequently, more pressure is generated due to the higher volume change ratio.

The piezoelectric actuators for all actuating modes is demanded to actuate large displacement and force output. That is, excellent electromechanical coupling characteristic is needed for the piezoelectric actuator in an inkjet printing application. It is noted that the poling process parameters play a crucial role in obtaining better electromechanical characteristics [10]–[12]. Therefore, shear mode piezoelectric actuators poled by various poling conditions were prepared and tested to obtain the optimal conditions. The design of poling electrodes was different from the conventional design [10]–[14], which has the poling direction along the plate-thickness direction of the actuator.

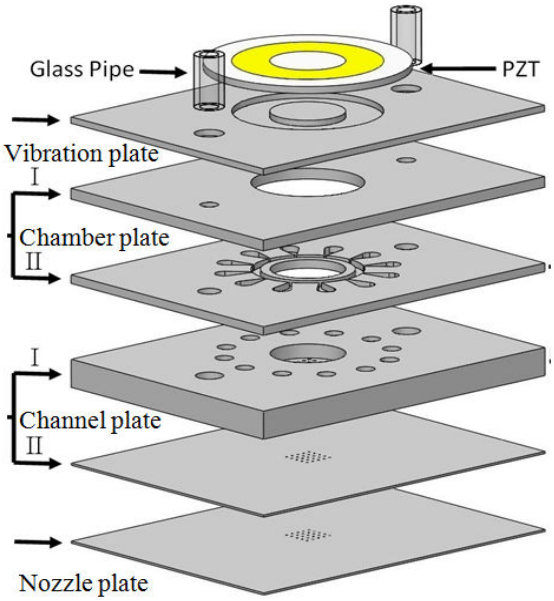

Fig. 2 Schematic of the microdroplet ejector

II. Design

Fig. 2 shows a novel microdroplet ejector with shear type piezoelectric actuator proposed in this study and its the cross-section view of the structure is shown in Fig. 3. The microdroplet ejector consists of several structural layers from bottom up: a nozzle plate, two channel plate, two chamber plate, and a shear type piezoelectric actuator. Those components are assembled to complete the ejector by gluing. The vibration plate has the two-level structure including the diaphragm and on which a bulge piled up. The shear mode piezoelectric actuator is glued on and suspended between the bulge and the surface of vibration plate. As an external field perpendicular to the poling direction is applied on the actuator, the induced shear effect make the diaphragm deflected through the rigid bulge. The thickness of bigger bulge, say 100μm, is larger than the 10μm thickness of the diaphragm. This design is considered to be capable of improving the volume sweep of the diaphragm. The volume sudden decrease in the pressure chamber causes droplets to be expelled from the orifice. The actuator disposed on the vibrating plate is shear acted under the effect of electric field, so as to promote the flat deformation of the vibrating block for varying the volume of the chamber. Thus the liquid in the chamber is uniformly sprayed from the nozzles owing to the flat deformation.

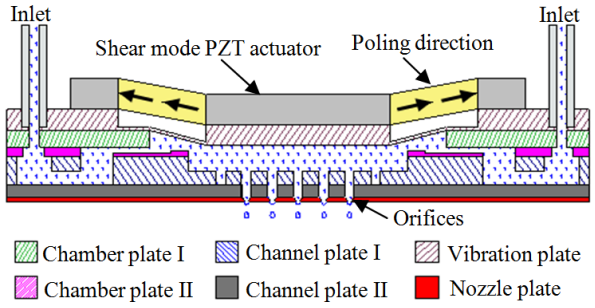

Fig. 3 The cross section view for the microdroplet ejector

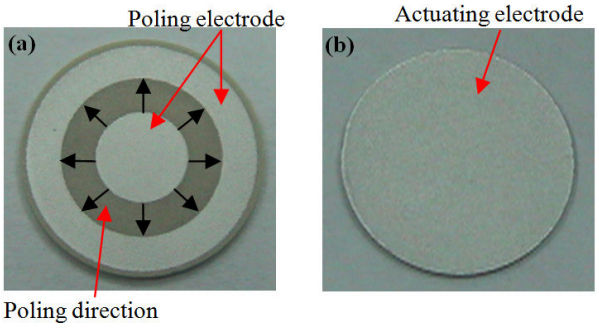

Fig. 4 Schematic of (a) poling electrode pattern and (b) actuating electrode pattern

III. Fabrication

A. Shear Mode Piezoelectric Actuator

The ferroelectric piezoelectric disc for the shear mode actuator was prepared by dry powder pressing technique using the commercial available piezoelectric powder (B1) from ARIOSE Company. This piezoelectric powder is widely used to make actuators due to its high electromechanical coupling coefficient and high Curie temperature. The powder had been baked for 2 hours in 120°C oven to remove the moisture before compacting. The powder mixture was placed into a die and compacted by applying a uniaxial pressure of 10MPa to generate the powder compact. The sintering process was performed in a tube furnace under a quiescent air atmosphere at a heating rate of 90 °C /min to the peak temperatures of 1250 °C for maintaining a duration of 2 hours, which followed by a 90°C /min cooling rate to the room temperature. The original dimensions of the green compact, 12mm in diameter and 1.2mm in thickness, were shrunk by 15% after sintering, and then

thinned to 0.4mm in thickness by polishing. The silver paste was then patterned to form the poling electrodes by a screen-printing technique, as shown in Fig. 4 (a). The piezoelectric disc was polarized by 6 kV in 120°C silicone oil bath with the time duration of 20min. The oil bath was then cooled to 60°C before the poling voltage was turned off. By applying actuating electrodes on the top and bottom surfaces of the plate actuator (Fig. 4 (b)), the actuating electric field (E) vertical to polarization direction (P) tended to result in shear deformation or out-of-plane displacement, as illustrated in Fig. 5.

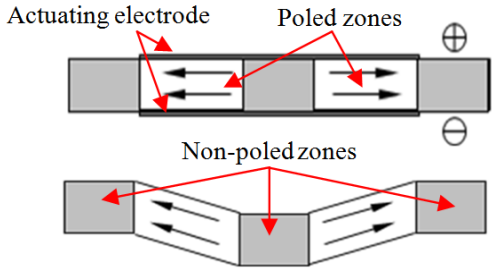

Fig. 5 Schematic of side view and shear mode deformation

B. Nickel Component

The four components in the microdroplet ejector were fabricated by multilevel electroforming technology. Both vibration plate and chamber plate II are electroformed with two-level structure, while the chamber plate I and nozzle plate have only a one-level structure. The polished circular plate made from stainless steel and 60 mm in diameter was the substrate for constructing these components. Four pieces with identical structures will be electroformed on a substrate. The AZ9260 positive tone photoresist was used as electroforming moulds, and nickel was the electroforming material. Two repeated steps including the mould patterning and the nickel electroforming are the main processes to construct levels of the component. Firstly, the substrate is patterned with photoresist as a mould. Secondly, the electroforming is performed by deposited nickel in the opening of the photoresist mould. The photoresist mould for each level cannot be removed until finishing the final level. After removing the mould by acetone, the electroformed components on the substrate can easily be taken off due to the medium adhesion. The nickel structure was deposited in a nickel sulfamate based electrolyte bath. An ac power supply was used with a cycle of 90 ms positive and 10 ms negative. First, a specific thick photoresist mould (AZ9260) was coated and patterned over the substrate. Next, a specific thick nickel layer was electrodeposited using a low-stress nickel sulfamate bath kept at a temperature of 46 °C with a pH value around 4. The current density was 2 A/dm^2. The average deposition rate was found to be 8 μm/h. A current density of 2 A/dm^2 appears to be suitable for electroforming the levels of the components, considering the surface roughness and internal stress. The fabricated vibration plate, chamber plate I, II, and nozzle plate are shown in Figs. 6~9.

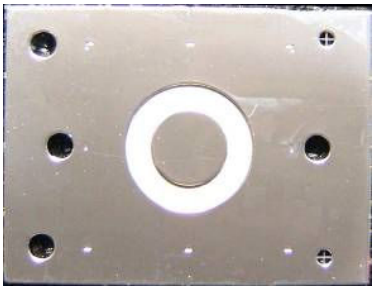

Fig. 6 The fabricated nickel vibration plate

Fig. 7 The fabricated nickel chamber plate I

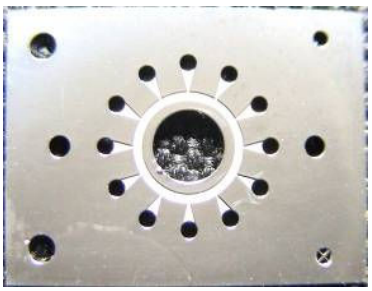

Fig. 8 The fabricated nickel chamber plate II

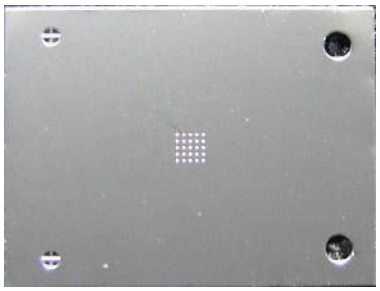

Fig. 9 The fabricated nickel nozzle plate

Figs. 10 (a) and (b) are the SEM picture of the vibration plate and cross-up view which shows the two-level structure. The bottom level is the diaphragm deposited first. Subsequently, the circular bulge is electroformed upwards on which piezoelectric actuator is attached. The diffuser channel that connects the buffer chamber and pressure chamber is electroformed in the second level with 35 μm thickness, as shown in Figs. 11 (a) and (b). The orifices in the nozzle plate were formed by the over deposition of nickel around the columnar photoresist mould. As the thickness of deposited nickel is larger than the height of the

columnar mould, lateral growth as well as height growth appear. The greater the over-deposition is, the smaller the nozzle orifice becomes. And, the development of the over deposition results in a paraboloid hole such as a nozzle, shown by the SEM picture in Figs. 12 (a) and (b).

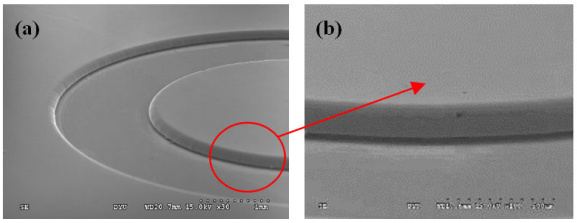

Fig. 10 SEM picture of the nickel vibration plate (a) and close-up view of the circular bulge (b)

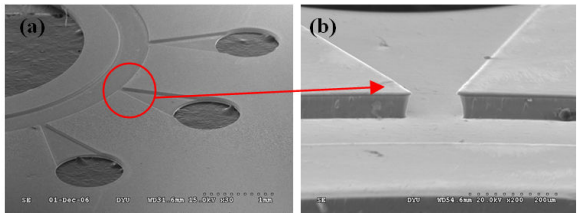

Fig. 11 SEM picture of the nickel chamber plate II (a) and close-up view of the diffuser channel (b)

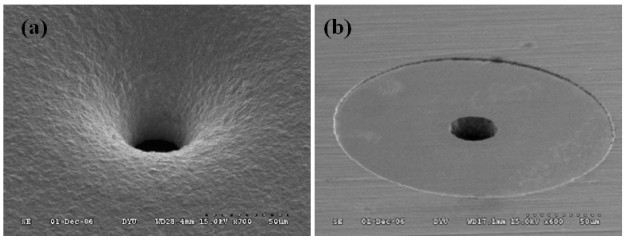

Fig. 12 SEM picture of bottom view (a) and top view (b) of the nickel orifice

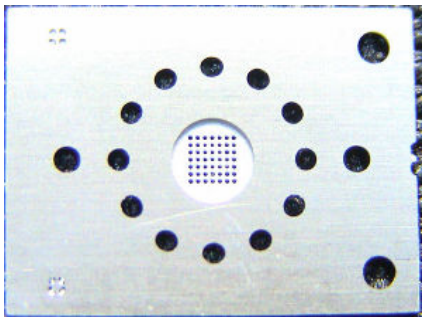

Fig. 13 The fabricated stainless steel top view of channel plate I

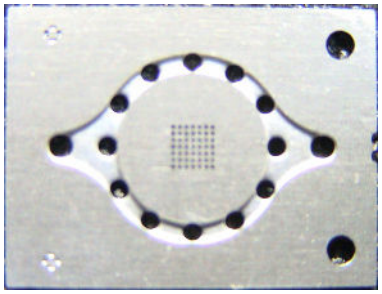

Fig. 14 The fabricated stainless steel bottom view of channel plate I

C. Stainless Steel Component

The channel plate I and II were made of the stainless steel manufactured using the MEMS-based lithography and etching process. An etchant consisting of 46g ferric chloride, 33g hydrogen peroxide and 54g deionized water were utilized to obtain smooth uniform channels and chamber on the stainless steel substrates. At the start, the AZ 9260 photoresist was coated on the stainless-steel substrate by spin coater with both spreading step and thinning step. The photoresist on the substrate was baked on a hot plate or in an oven, and then exposed by a standard UV mask aligner (Karl Suess MA-6). The UV exposure process was performed under the hard contact mode with an intensity of 6mW/cm^2 at a wavelength of 365 nm. The exposed photoresist was then developed in an immersion process via AZ400K diluted developer. Finally, the samples that were wet etched were immersed in the etchant at 53-58^{o}C. The fabricated top and bottom view channel plate I and channel plate II are shown in Figs. 13~15. Figs. 16 (a) and (b) are the SEM picture of the channel plate I and close-up view of the circular channel. Figs. 17 (a) and (b) are the SEM picture of the channel plate II and close-up view of the circular channel.

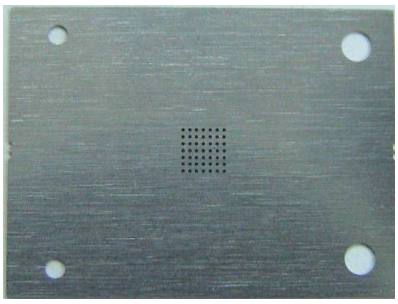

Fig. 15 The fabricated stainless steel channel plate II

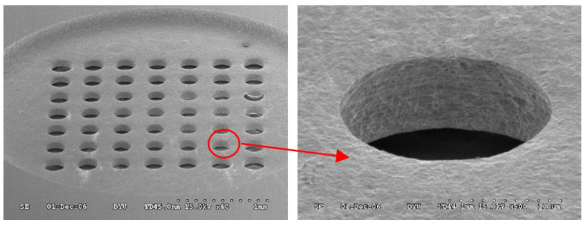

Fig. 16 SEM picture of the stainless steel channel plate I (a) and close-up view of the circular channel (b)

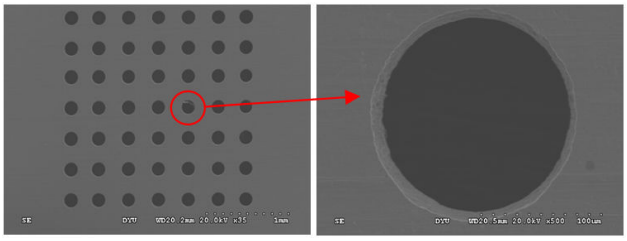

Fig. 17 SEM picture of the stainless steel channel plate II (a) and close-up view of the circular channel (b)

D.Assembly

After nickel electroforming and stainless steel etching all levels of the six kinds of components for the microdroplet ejector, their structures were observed and checked by SEM (JEOL JSM-6360). At first, applying epoxy adhesive (CIBA-GEIGY, AV 119) on the attached surfaces by screen printing, six components (Vibration, chamber I II, channel I, II, and nozzle plate) with aligned marks were assembled by a CCD aligning system. The adhesive was cured in the oven kept at 120°C for 2 hours. Then, the piezoelectric actuator was attached by another epoxy adhesive (3M, DP-460) cured at a lower temperature of 60 ℃ for 2 hours to avoid depolarization. Finally, the two inlet tubes were connected to the microdroplet ejector inlet ports. Fig. 18 shows the photo of the assembled microdroplet ejector device.

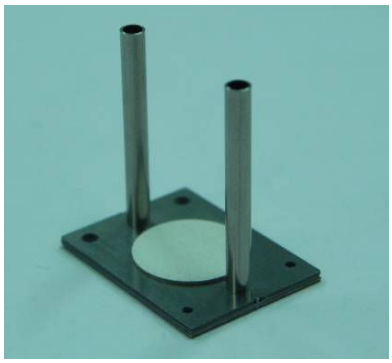

Fig. 18 The assembled microdroplet ejector

IV. Piezoelectric Actuator Performance

Samples were driven by ac 100Vpp voltage at a frequency of 1 kHz, far below the resonant frequency, and measured by the two-dimensional scanning laser vibrometer (Polytec MSV300) to obtain their actuated displacements. Each obtained data is the average value from the three measured samples with the same conditions. The actuated displacement for the shear mode actuator of a given dimension depends on the known shear piezoelectric coefficient (d_{15}). The higher the shear piezoelectric coefficient is, the larger the actuated displacement results. If the sample coefficient is unknown, then it can be evaluated by the actuated out-of-plane displacement measured under a certain actuating electric field. Fig. 19 displays the instrument configuration for measuring the actuated displacement of the shear mode piezoelectric actuator. The nickel substrate with trench of 7 mm in diameter of circle was bonded to the transparent glass and used as a testing fixture for displacement measurement, as shown in Fig. 20. The only active region of the actuator was the suspended part. The ac input voltage will induce alternatively upward and downward deformations. And its out-of-plane displacements on the three paths are plotted as three curves in Fig. 21.

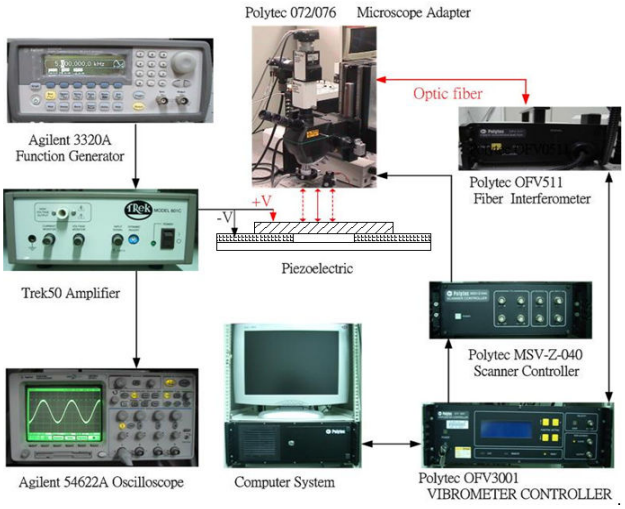

Fig. 19 Configuration of instruments for measuring the actuated displacement of the shear mode piezoelectric actuator

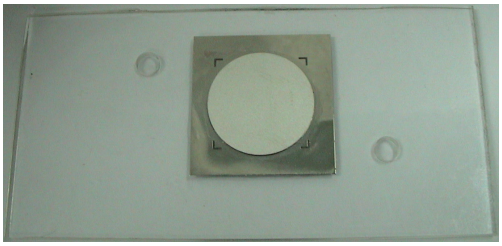

Fig. 20 Schematic of the shear mode piezoelectric actuator bonded on a silicon substrate with a trench

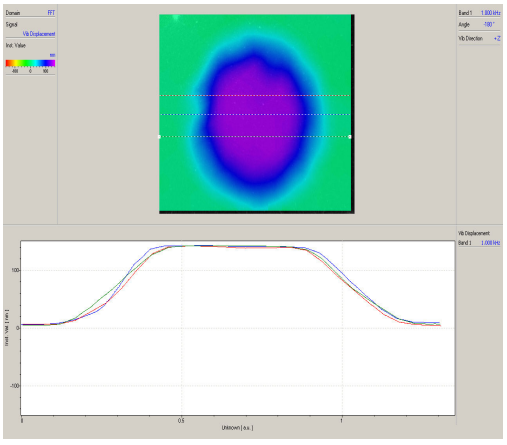

Fig. 21 Measured deformations of path distributions of the out-of-plane displacement at 100 Vpp ac input voltage

V. Experimental Observations

An experimental system was set up to observe the droplet ejection process at different time instants and to measure the diameter of the droplets. The experimental apparatus consists of an available microdroplet ejector, an electronic system, and an image capturing system, as shown in Fig. 22. A LED is placed under the microdroplet ejector to side-illuminate the microdroplet stream. The ejector is arranged to eject droplets vertically under influence of gravity. Two signals, synchronized with adjustable time delay, are sent to the ejector and the LED, respectively. The driving waveform consisted of five segments. The initial segment had voltage rise to 70V in 4 μs, which created a chamber expansion. The maximum voltage was held for 12 μs in the next segment to propagate and stabilize fluid wave. The following segment with the voltage driven to −70V in 3 μs induced fluid compression and propagation to the orifice for ejecting droplets. Before the voltage was returned to ground, it was held at −70V for 6 μs to propagate the fluid compression wave. Shifting voltage to zero in 4 μs for cancelling compression wave, the fluid was pulled back with the liquid surface settled at the nozzle orifice. Fig. 23 shows a microdroplet ejection sequence of the array ejector. During the droplet flight, the visualized droplet size was around 40 μm in diameter.

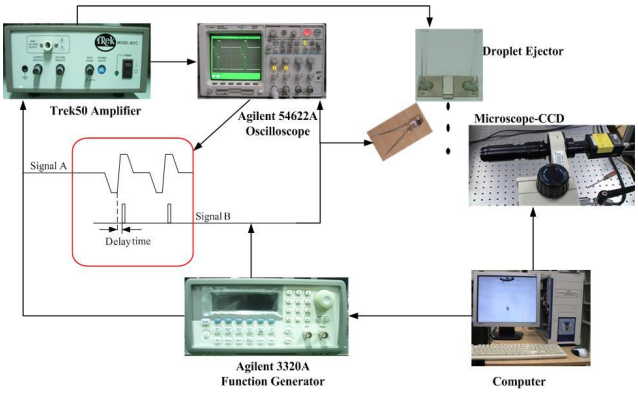

Fig. 22 Schematic view of the optical system for microdroplet ejection visualization

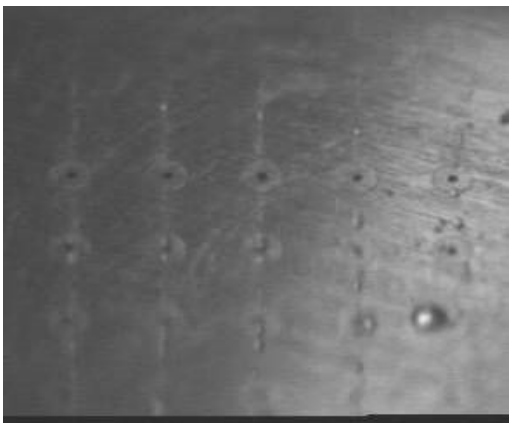

Fig. 23 Microdroplet ejection situation of the array ejector

VI. Conclusion

A novel design of shear mode piezoelectric actuating module used for microdroplet ejector or inkjet head is proposed. The components for a novel microdroplet ejector were successfully fabricated by UV LIGA technology and stainless steel etching. The crucial nozzle structure was realized by the lateral growth of over deposition onto the columnar mould. The shear mode piezoelectric actuator was successfully fabricated with actuated displacement as expected and would be applied in the novel actuating module of the microdroplet ejector.

Acknowledgment

The authors would like to thank the National Science Council of the Republic of China, Taiwan for financially supporting this research under Contract No. NSC-95-2221-E-212-037-MY2.

References

[1] Y. Fuda, T. Yoshida, Piezoelectric torsional actuator, Ferroelectrics 160 (1994) 323–330.
[2] J. Satonobu, N. Torii, K. Nakamura, S. Ueha, Construction of megatorque hybrid transducer type ultrasonic motor, Jpn. J. Appl. Phys. 35 (1996) 5038–5041.
[3] E.L. Kyser, S.B. Sears, Method and apparatus for recording with writing fluids and drop projection means therefore, US Patent 3,946,398 (1976).
[4] T. Kitahara, Ink-jet head with multi-layer piezoelectric actuator, in: Proceedings of the IS&T's 11th International Congress on Adv. in Non-Impact Printing Technologies, Hilton Head, SC, USA, October 29–November 3, 1995, pp. 346–349.
[5] S.I. Zoltan, Pulse droplet ejection system, US Patent 3,683,212 (1974).
[6] A.J. Michaelis, A.D. Paton, S. Temple, W.S. Bartky, Droplet deposition apparatus, US Patent 4,887,100 (1989).
[7] K.H. Fischbeck, P.A. Hoisington, Shear mode transducer for ink jet systems, US Patent 4,825,227 (1989).
[8] J. Brunahl, A.M. Grishin, Piezoelectric shear mode drop-on-demand inkjet actuator, Sens. Actuators A 101 (2002) 371–382.
[9] http://www.dimatix.com/technology/spectra-piezoelectric.asp.
[10] D.A. Berlincourt, C. Fall, F.T. Brunarski, Polarization of titanate ceramics, US Patent 2,928,163 (1960).
[11] J.A. Sugden, Ferroelectric ceramic materials, US Patent 3,068,177 (1962).
[12] M. Sayer, B. Judd, K.E. Assal, E. Prassad, Poling of piezoelectric, J. Can. Ceram. Soc. 50 (1981) 23–28.
[13] P. Bryant, Optimization of poling conditions for piezoelectric ceramics, Mater. Sci. Forum 34 (1988) 285–289.
[14] H.T. Chung, H.G. Kim, Characteristics of domain in tetragonal phase PZT ceramics, Ferroelectrics 76 (1987) 327–333.